ASPECTS REGARDING SF6 SWITCH DISCONNECTOR FRAMEWORK DESIGN

Liviu **NEAMT**, Olivian **CHIVER,** Zoltan **ERDEI,** Cristian **BARZ**
Technical University of Cluj-Napoca
liviu.neamt@cunbm.utcluj.ro

Keywords: Finite element analysis; high-voltage techniques; switchgear

Abstract*: The complexity of the designing process of a switch disconnector framework comes from the almost impossible task to appreciate the discrepancy between the ideal and practical electric strength. Complicated geometries characterized by nonuniform fields are predesigned based on a set of analytical relations and corrected/optimized based on numerical methods and high voltage testing on prototypes. This paper suggest some approaches to minimize the effort and the steps required to achieve an acceptable stainless steel housing, in the insulators area, for a medium voltage SF_6 switch disconnector. The results are based on simple analytical evaluation and finite element analysis in both 2D and 3D configurations.*

1. INTRODUCTION

The commutation in SF_6, alongside that in vacuum are, nowadays, the basis of the power system technology [1], [2]. The switchgears have to be continuously improved regarding their safety, endurance, operating simplicity, capability of integration in smart grids and availability for higher and higher voltages and currents. All these demands constitute the input data for design process, which is carried out through an analytical methodology. The result, the prototype is subject of improving and validation based on a set of standardized tests in accordance with its rated parameters. Actual development of virtual reality, offers a faster and cheaper way to improve/validate an analytical pre-sized configuration, avoiding the prototyping steps until the final validation. The numerical methods for solving any type of engineering problems are affordable and a right use of them, guarantees results comparable

with real tests. Finite element analysis (FEA) is one of the most powerful tools for electric field computation with good results in electrical apparatus simulation, [3-6].

In this paper the dielectric design of the stainless steel housing is studied in the insulators area, for an indoor, 24 kV rated voltage, 630 A rated current, switchgear, filled with 0.15 MPa pressure SF_6.

The dielectric design is conducted on breakdown in uniform and weakly nonuniform fields. The "practical electric strength" of the SF_6 for given structure is, [7]:

$$E_b = \left(\frac{E_b}{p}\right)_t \cdot (10 \cdot p)^z \quad [kV/cm] \tag{1}$$

$(E_b/p)_t$ in KV/(cm·MPa) is the "technical relative strength", p in MPa is the pressure of the insulated gas and z is a factor introducing different types of applied voltages. For a positive lightning impulse (1.2/50 μs), $(E_b/p)_t$ = 80 KV/(cm·MPa) and z = 0.8, [7]. The result becomes 110.65 KV/cm.

Imposing the standardized voltage for impulse testing, [8], V_{imp} = 125 KV, the minimum insulation distance could be determined as:

$$d = \frac{V_{imp}}{E_b \cdot e_r \cdot e_{max} \cdot \eta} \quad [cm] \tag{2}$$

Variable e_r is the roughness factor, here considered as 0.75, covering technical mean roughness, [7], [9], [10]; e_{max} is the curvature factor, equal to 1.1 for an inner radius of the electrode equal to 9 mm, [7]; η is the Schwaiger factor or the degree of uniformity close to 0.23 for the desired configuration [7]. The computation goes to a value of 6 cm for minimum insulation distance.

In above conditions the corrected practical electric strength is:

$$E_b = E_b \cdot e_r \cdot e_{max} \quad [kV/cm] \tag{3}$$

with a value of 91.2 KV/cm which must be satisfied in all regions inside of the switchgear tank.

2. INVESTIGATED CONFIGURATIONS

The insulators are 230 mm spaced and the inner cooper rod is 18 mm diameter, Figure 1 (a). The geometries of the upper side of the housing are started with a flat configuration, which will be bent between up to a flip angle of 120° to create a compact structure, Figure 1 (b). Also, based on actual solution for stiffen the insulators against rotation (two linear carvings cut out into insulators and also in the housing), the bushing diameter is another parameter tested for its influence on electric filed intensity, Figure 2. The insulators design is not the subject of this paper, only the influences of the above characteristics are investigated, so the relevant results will constitute the trends, rather than absolute values.

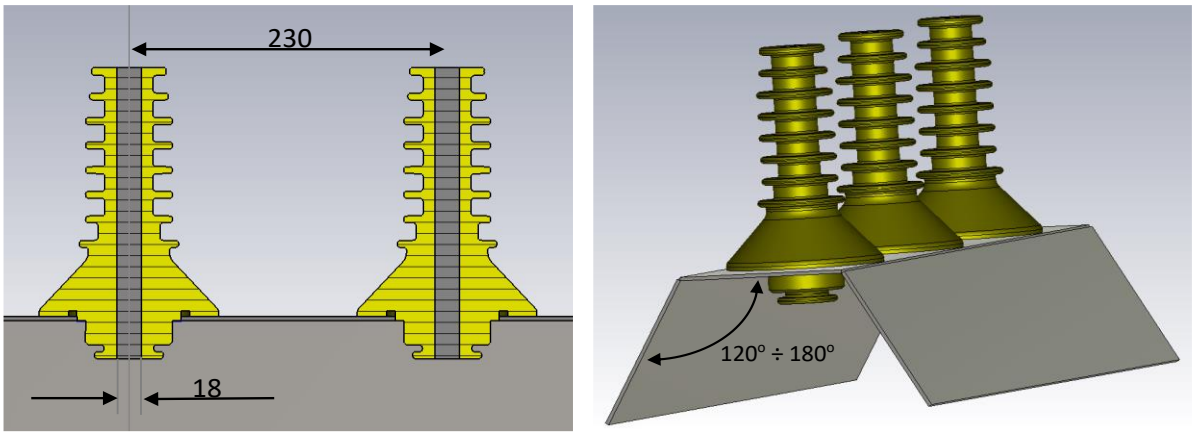

(a) *(b)*

Fig. 1. (a) The insulators geometry; (b) The upper side of the housing with mounted insulators.

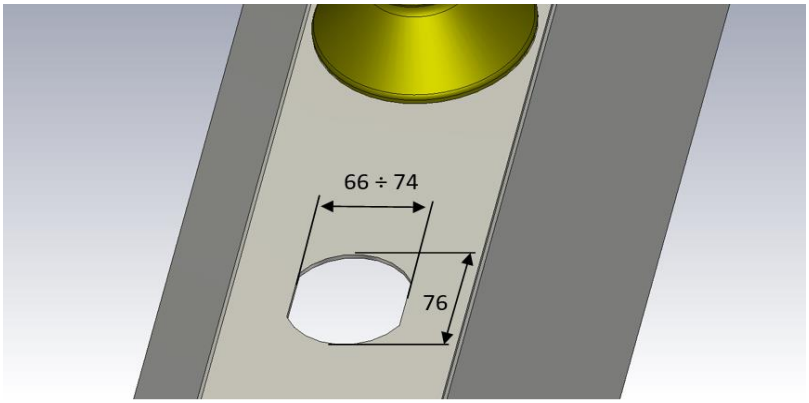

Fig. 2. The solution for stiffen the insulators against rotation.

2.1. Bushing diameter

For a preliminary computation of the bushing diameter, a coaxial cylindrical capacitor configuration will offer the electric field intensity values to be compared to the practical electric strength.

The major problem of the insulator passing through the housing is that always some space will remain between the metal frame and the insulators, so above capacitor will be with two dielectric layers, one consisted by epoxy resin, relative permittivity equal to 3 and the other, very thin, filled with SF_6, having the dielectric constant equal to 1.00203, Figure 3.

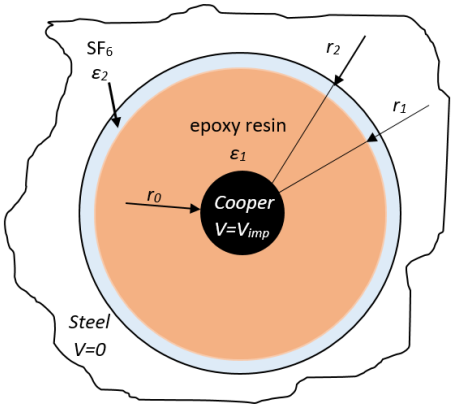

Fig. 3. Insulator crossing the upper side of the housing.

The values of the electric field in each point of the configurations could be computed based on:

$$E(r_i) = \frac{V_{imp}}{\varepsilon_i \cdot r_i \left(\frac{1}{\varepsilon_1} ln\frac{r_1}{r_0} + \frac{1}{\varepsilon_2} ln\frac{r_2}{r_1}\right)} \quad (4)$$

Selecting the value of r_2-r_1 < 0.1 mm, the minimum bushing diameter which goes to satisfy the practical electric strength is 65 mm. For this value, the electric field intensity on the exterior of the insulator reach a magnitude of 90 KV/cm. Keeping in mind that assessment of the roughness factor and the curvature factor is not very rigorously, the minimum distance between the cooper rod and the framework will be considered 66 mm. This distance will be the distance between carvings that stiffen the insulators against rotation. As conclusion the bushing diameter must be above 66 mm. To have a larger interval of variations, i.e. 66 to 74 mm, this goes to a ratio of lower area of insulator of 38 mm, Figure 2.

The next step is to perform different carvings on cylindrical models Figure 3, and analyze its influence on dielectric stress. For the beginning 2D planar problems are solved using David Meeker's Finite Element Method Magnetics, FEMM, [11]. For 72 mm between linear carvings, the electric field distribution looks like in Figure. 4.

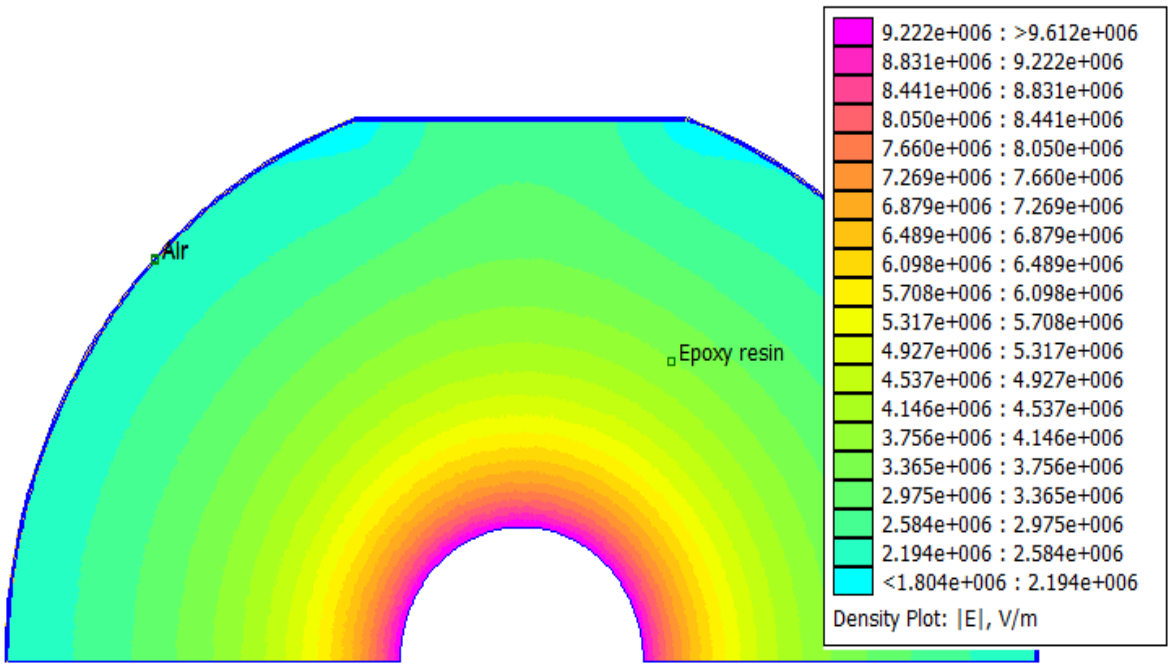

Fig.4. Electric field distribution.

The total computing time is approx. 2.5 minutes for 1669993 elements. The refinement process to achieve a good balance between accuracy versus the number of finite elements, i.e. computing time and hardware resources, was performed based on coaxial cylindrical configuration.

Due the speed of analyses it can be ran a very important number of FEA. The results are presented in Figure 5.

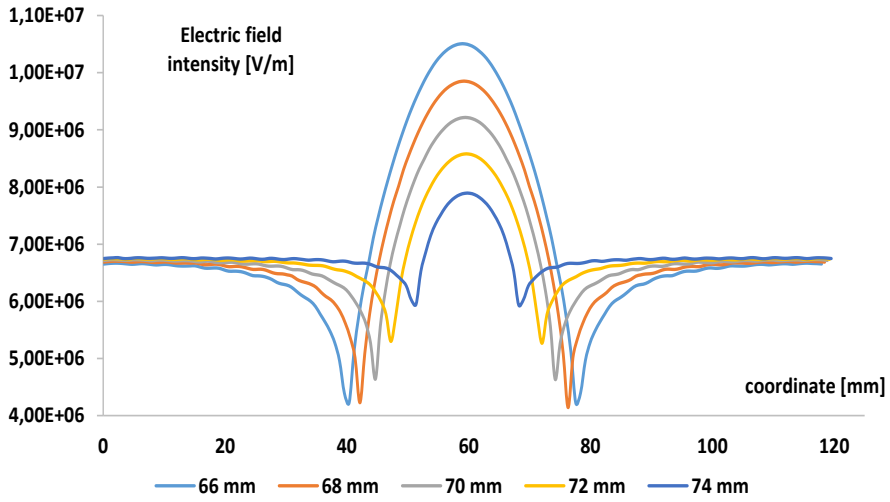

Fig.5. Electric field intensity on boundary between insulator and SF_6, for different insulator carvings in 2D FEA.

For 70 mm between carvings, the electric field is bigger than 92 KV/cm, a value bellow 90 KV/cm appears for 72 mm distance.

2.2. 3D FEA

Of course a 2D FEA do not reflect the real electric field distribution. 3D analyses must be done to take into account the entire region geometry. The configurations from Figures 1 and 2, with a test voltage applied to middle rod, all other conductive parts being putted to the earth, were considered.

The electrostatic FEA are performed using CST Studio Suite 2015, [12]. Approximatively 37.800.000 initial hexahedral cells are used with 10^{-12} solver accuracy and 2 refinement steps. The final number of mesh cells reached approx. 64.500.000, Figure 6 (a). On an Intel® Core™ i5 – 4590 CPU, 32 GB RAM based system, for one configuration the solving time is 1 hour and 32 minutes for 1070 iterations, Figure 6 (b).

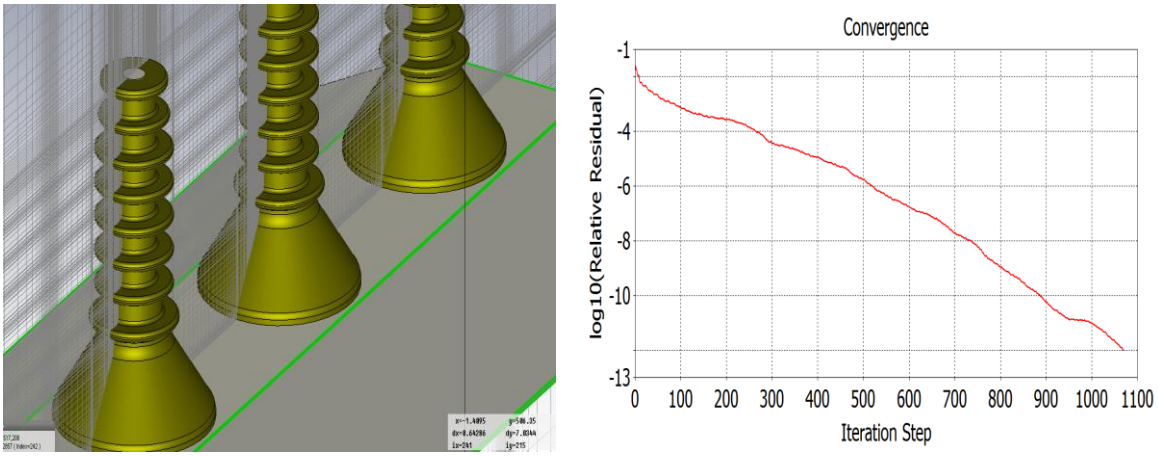

(a) *(b)*

Fig. 6. (a) Refined mesh; (b) Convergence versus iterations.

The potential and the electric field intensity in entire configuration are analyzed. In Figures 7 (a) and (b) there are presented the distributions of above variables in a longitudinal cutting plane for a bending angle of 160° and 72 mm between linear carvings.

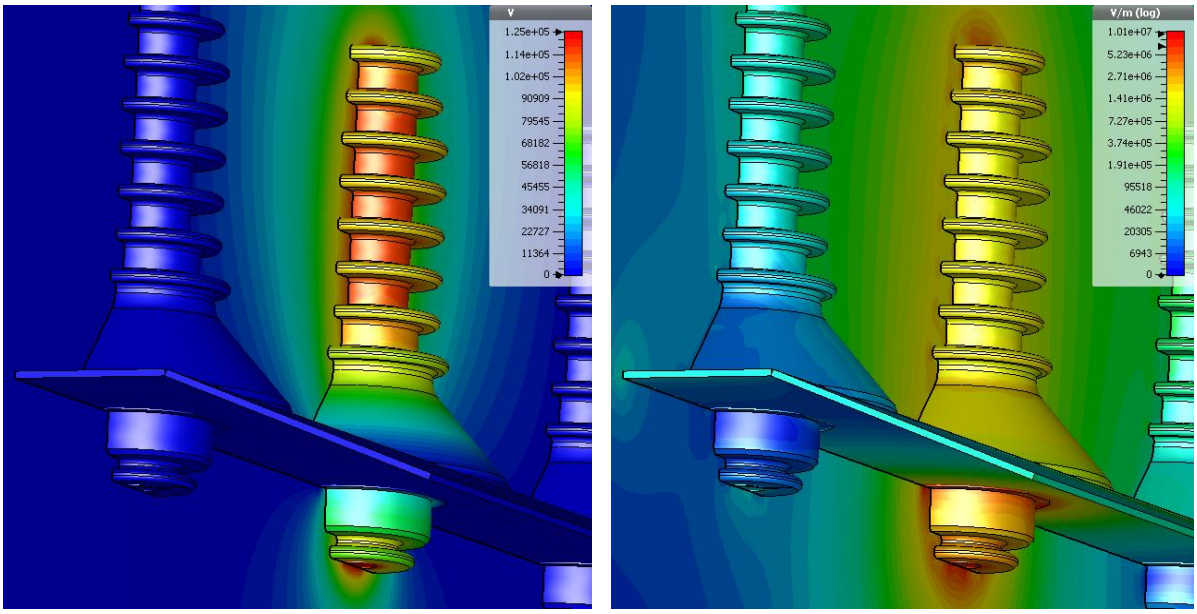

(**a**) (**b**)

Fig. 7. (a) The potential distribution in the longitudinal cutting plane; (b) The electric field intensity distribution in the longitudinal cutting plane.

For a transversal cutting plane through the middle insulator, the distributions of the potential and of the electric field intensity are shown in Figures 8 (a) and (b). The red areas from electric field distributions are more electric stressed and these portions must be evaluate in detail.

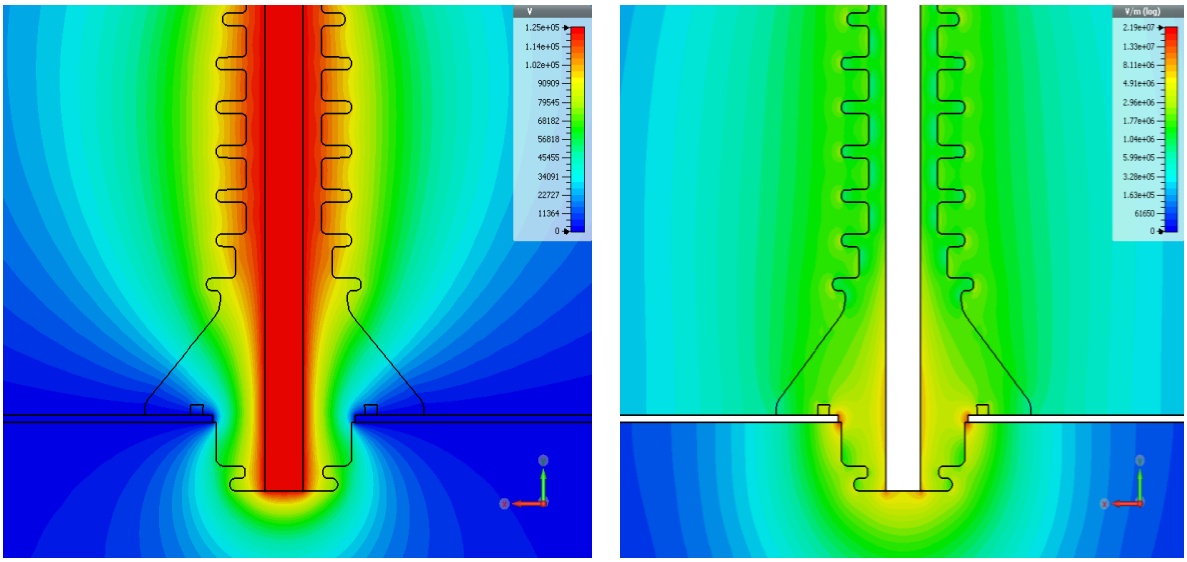

(a) *(b)*

Fig.8. (a) The potential distribution in the transversal cutting plane; (b) The electric field intensity distribution in the the transversal cutting plane.

Figures 9 and 10 show the electric field intensity variations for all analyzed geometries. First, in Figure.9 is the electric field intensity for different insulators carvings and in Figure 10 is the electric field intensity, for different bending angle of the upper side of the housing. Remembering the computed value of the practical electric strength, (2) equal to 91.2 KV/cm the interpretation becomes simple and logically.

It can be seen that, for 66 up to 72 mm, the influence of the linear curving is very important and determines the maximum dielectric stress. For an electric field above the corrected practical electric strength, (2), this will lead to breakdown. As it can been seen from Figure 9 for bigger values than 72 mm, this influence vanishes. Due this fact, the configuration with 72 mm between carvings is kept for the next analyses.

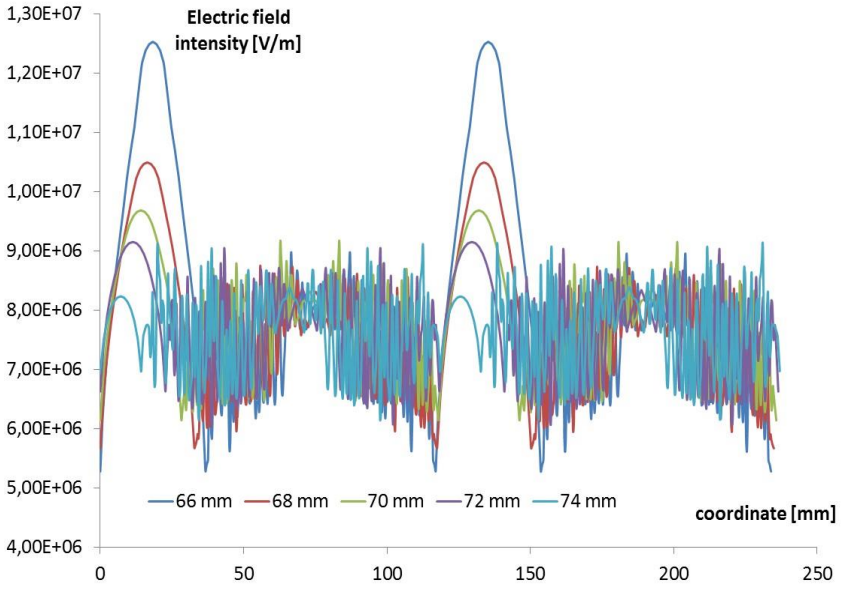

Fig. 9. Electric field intensity for different insulators carvings.

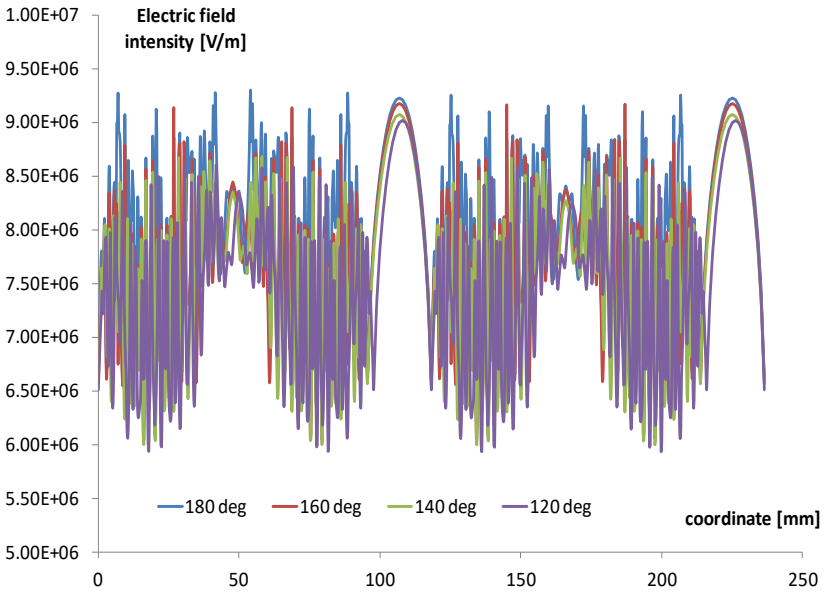

Fig.10. Electric field intensity for different bending angle of the upper side of the housing.

The bending angle has a very little influence on electric field intensity, causing a slightly reduction of it, following the variation from 180^o to 120^o, Figure 10.

3. CONCLUSIONS

Toward the method presented in [13], there are some improvements proposed in this paper. Consequently, to minimize the effort required to achieve an acceptable stainless steel housing, in the insulators area, for a medium voltage SF_6 switch disconnector, we propose the next algorithm:

- First of all, a 2D planar coaxial cylindrical capacitor configuration is created for computing the initial bushing diameter,
- The same structures, but with different carvings added to insulators, for stiffen them against rotation, are analyzed on a 2D Finite element environment,
- Only the solutions that fulfilled the dielectric requirement will be forwarded to 3D FEA for final validation/optimization.

The succession of: simple analytical, 2D FEA and 3D FEA offer the solutions of the problem in an efficient manner, regarding the computing time and the elimination process for inadequate configurations.

Based on FEA it is very simple and accurate to predict the dielectric behavior of the future prototype and some vulnerability can be corrected before the production phase. Also "countless" scenario regarding the geometries, materials and different applied voltages could be considered inside of the virtual environment.

Of course the electrostatic simulation is only one step, other electromagnetic, mechanic, thermal, etc. analyses could be performed and the results would generate a full and complex assembly of the future switchgear behaviors. The output of the process will be not just an available device, accordingly to standards, but could be also a close to optimum one.

REFERENCES

[1] R. Smeets, L Sluis, M. Kapetanovic, D. Peelo and A Janssen, *Switching in Electrical Transmission and Distridution Systems*, John Wiley & Sons, Ltd., 2015.

[2] D. Peelo, *Current Interruption Transients Calculation*, John Wiley & Sons, Ltd., 2014.

[3] M. Szewczyk, W. Piasecki, M. Wronski, and K. Kutorasinski, *New Concept for VFTO Attenuation in GIS with Modified Disconnector Contact System*, IEEE Transactions on Power Delivery, vol.30, no.5, pp. 2138-2145, Oct. 2015.

[4] X. Wei, Z. Peng, Z. Deng, H. Wu, Q. Wang and C. Wang, *Research on the influence of different defects upon GIS disconnector electric field distribution*, Proceedings of the 11th International

Conference on the Properties and Applications of Dielectric Materials, pp.588-591, 2015.
[5] M. Stosur, M. Szewczyk, W. Piasecki, *GIS disconnector switching operation VFTO study*, Proceedings of the International Symposium, Modern Electric Power Systems (MEPS), Wroclaw, Poland, pp.1-5, 2010.
[6] J.Y. Xu, L. Lu, S. Lin, *Numerical Analysis of Electric Field of 1100 kV Disconnector in GIS*, High Voltage Engineering, vol. 34, pp. 2102-2106, 2008.
[7] R. Arora and W. Mosch, *High Voltage and Electrical Insulation Engineering*, Wiley-IEEE Press, 2011.
[8] EN 62271/1, *High-voltage switchgear and controlgear-Part 1: Common specifications*, 2007.
[9] M. Bujotzek, M. Seeger, *Parameter dependence of gaseous insulation in SF6*, IEEE Transactions on Dielectrics and Electrical Insulation, vol.20, no.3, pp.845-855, June 2013.
[10] M. Seeger, M. Bujotzek and L. Niemeyer, *Formative time lag and breakdown in SF6 at small protrusions*, Proceedings of the 17th International Conference on Gas Discharges and Their Applications, GD 2008., Cardiff, pp. 317-320, 2008.
[11] Finite Element Method Magnetics, http://www.femm.info/wiki/HomePage.
[12] CST Studio Suite, https://www.cst.com/.
[13] L. Neamt, O. Chiver, Z. Erdei, C. Barz, *Considerations about medium voltage SF6 switch disconnector framework design based on 3D electrostatic FEA*. Proceedings of the 2016 IEEE 16th International Conference on Environment and Electrical Engineering (EEEIC), Firenze, Italy, 7–10 June 2016, pp 1-4